Controlled synthesis of PbS–Au nanostar–nanoparticle heterodimers and cap-like Au nanoparticles

Nana Zhao, Lianshan Li, Teng Huang and Limin Qi*

Received 6th June 2010, Accepted 28th July 2010
DOI: 10.1039/c0nr00385a

Uniform PbS–Au nanostar–nanoparticle heterodimers consisting of one Au nanoparticle grown on one horn of a well-defined six-horn PbS nanostar were prepared using the PbS nanostars as growth substrates for the selective deposition of Au nanoparticles. The size of the Au nanoparticles on the horns of the PbS nanostars could be readily adjusted by changing the PbS concentration for the deposition of Au nanoparticles. An optimum cetyltrimethylammonium bromide concentration and temperature were essential for the selective deposition of uniform Au nanoparticles on single horns of the PbS nanostars. Unusual PbS–Au nanoframe–nanoparticle heterodimers were obtained by etching the PbS–Au nanostar–nanoparticle heterodimers with oxalic acid while novel cap-like Au nanoparticles were obtained by etching with hydrochloric acid. The obtained heterodimeric nanostructures and cap-like nanoparticles are promising candidates for anisotropic nanoscale building blocks for the controllable assembly of useful, complex architectures.

Introduction

Remarkable success has been achieved in the controlled synthesis of single-component nanocrystals with tailored dimensions and morphologies in the past decade.[1–6] Recently, well-defined nanocrystal heterostructures or hybrid nanostructures containing discrete domains of different components have attracted increasing interest because of their multiple functionalities and enhanced performance.[7–11] Among the various hybrid nanostructures, nanocrystal heterodimers consisting of two adjacent domains made of different materials are highly desirable in a wide range of applications.[12–19] Generally, such heterodimeric nanostructures can integrate several different functionalities in one nanoobject to the meet requirements for diverse applications; furthermore, the close coupling of two different components at the nanoscale might significantly improve the performance, or even generate new properties. For example, dumbbell-like, Fe_3O_4–Au heterodimeric nanostructures were demonstrated to be a dual-functional probe useful for simultaneous optical and magnetic imaging,[20a] as well as a multifunctional platform for target-specific platin delivery;[20b] whereas Fe_3O_4–Ag heterodimer nanoparticles serve as a bifunctional nanomaterial for two-photon fluorescence imaging and magnetic manipulation.[21] Semiconductor–metal heterodimeric nanostructures are a classic example since metal nanoparticles on the surface of semiconductors can improve the charge separation in semiconductors and can also alter the optical properties of semiconductors, particularly their photoluminescence quenching or enhancement.[9,22,23] For instance, for Au-tipped CdSe nanorods, strong mixing of the semiconductor and metal electronic states leads to a modified density of states, thereby exhibiting broadened energy levels and a reduced bandgap.[24] The charge-separated state in CdSe–Au nanorods has been utilized for the photoreduction of an acceptor molecule, which offers a promising route for converting solar energy into chemical energy.[25] In addition, heterodimeric nanostructures are promising anisotropic building blocks for the controllable assembly of useful, complex architectures.[26] To date, a number of nanoscale heterodimers based on various combinations of metals, oxides and chalcogenides have been synthesized. However, it remains a great challenge to develop facile routes toward high-quality heterodimeric nanostructures with increasing degrees of complexity and functionality.

As a narrow-bandgap semiconductor, PbS shows extensive quantum-size effects in nanocrystalline form, and considerable attention has been paid to the controlled synthesis of PbS nanocrystals because of their wide-ranging potential applications, such as in near-IR communication, optical switches, thermal and biological imaging, and solar cells.[27–31] Meanwhile, Au nanoparticles have been the focus of intense research owing to their optical, electronic, and chemical properties and promising applications in nanoelectronics, biomedicine, sensing and catalysis.[32] Great effort has been devoted to the morphology-controlled synthesis of Au nanostructures since the shape and size of Au nanostructures considerably influences their properties and relevant applications.[2–4,33] In particular, Au nanocaps or semishells have stimulated considerable interest because of their novel optical and plasmonic properties.[34] It is therefore interesting to synthesize PbS–Au heterodimeric nanostructures with controlled architectures. Notably, monodisperse PbS nanospheres were used as growth substrates for gold deposition, leading to the formation of PbS–Au_1, PbS–Au_4, and PbS–Au_n heterogeneous nanostructures *via* preferential deposition on PbS facets with the highest reactivity.[18] Recently, hollow PbS_x solid Au heterodimeric nanostructures were successfully synthesized through a mild reaction between PbS nanospheres and the gold species in the presence of dodecylamine.[19] However, the thus-far

Beijing National Laboratory for Molecular Sciences, State Key Laboratory for Structural Chemistry of Unstable and Stable Species, College of Chemistry, Peking University, Beijing 100871, P. R. China. E-mail: liminqi@pku.edu.cn

obtained PbS–Au heterodimers are always constructed as spherical or cubic PbS nanocrystals. It would be desirable to explore the synthesis of nanoscale PbS–Au heterodimers consisting of well-defined PbS nanocrystals with complex shapes.

Herein, well-defined, star-shaped PbS nanocrystals with six horns were used as the growth substrate for the selective deposition of Au nanoparticles on one horn of the PbS nanostars, leading to the formation of unique PbS–Au nanostar–nanoparticle heterodimers. After etching the heterodimers with different acids, unusual PbS–Au nanoframe–nanoparticle heterodimers and cap-like Au nanocrystals could be readily obtained.

Experimental

Synthesis of PbS nanostars

PbS nanostars were prepared in aqueous solutions of mixed cationic/anionic surfactants following a method reported previously.[30] In brief, 3 mL of water, 0.5 mL of 0.05 M cetyltrimethylammonium bromide (CTAB), 0.1 mL of 0.05 M sodium dodecyl sulfate (SDS), and 0.4 mL of 1 M acetic acid were mixed at room temperature, followed by the addition of 0.2 mL of 0.5 M $Pb(OAc)_2$ and 0.2 mL of 0.5 M thioacetamide (TAA) under stirring, giving concentrations of 5.7 mM and 1.1 mM for CTAB and SDS, respectively. The resultant translucent solution was thermostated at 80 °C for a certain time under static conditions, resulting in a brown colloid solution. The colloidal particles were collected by centrifugation, which could be redispersed well in water. For the synthesis of nanostars with sharp horns, 0.022 M NaCl was added to the synthesis solution with other conditions essentially unchanged.

Synthesis of PbS–Au nanostar–nanoparticle heterodimers and their etching by acids

Typically, 0.1 mL of 0.01 M $HAuCl_4$ and 160 μL of 0.1 M ascorbic acid was added to 2.38 mL of 0.1 M CTAB under stirring. Then, 300 μL of aqueous PbS dispersion containing 5.66 mM PbS was added into the mixed solution, giving concentrations of 0.065 M for CTAB, 0.28 mM for $HAuCl_4$, 4.4 mM for ascorbic acid, and 0.48 mM for PbS. After stirring, the solution was incubated at 27 °C for ~12 h. The products were collected by centrifugation and washed with ethanol and water. The obtained PbS–Au nanostar–nanoparticle heterodimers were put into 0.05 M oxalic acid and 6 M hydrochloric acid to dissolve PbS, resulting in the formation of PbS–Au nanoframe–nanoparticle heterodimers and cap-like Au nanoparticles, respectively.

Characterization

The products were characterized by scanning electron microscopy (SEM, Hitachi S 4800, 15 kV), transmission electron microscopy (TEM, JEOL JEM-200CX, 160 kV), high-resolution TEM (HRTEM, FEI Tecnai F30, 300 kV), X-ray diffraction (XRD, Rigaku Dmax-2000, Ni-filtered Cu Kα radiation), and UV–vis spectroscopy (Perkin Elmer Lambda 35).

Results and discussion

Uniform, well-defined, star-shaped PbS nanocrystals with six horns were synthesized using the method we previously developed, as shown in Fig. 1a. The synthesis of PbS–Au nanostar–nanoparticle heterodimers with a Au tip on one horn was achieved by the reduction of $HAuCl_4$ with ascorbic acid in an aqueous dispersion of PbS nanostars in the presence of CTAB. Fig. 1b shows a typical TEM image of the PbS–Au heterostructures obtained with a PbS concentration of 0.48 mM at 27 °C, indicating the exclusive formation of uniform nanostar–nanoparticle heterodimers consisting of PbS nanostars ~80 nm and gold nanoparticles ~50 nm. An enlarged TEM image is shown in Fig. 1c, which clearly shows that one gold nanoparticle preferentially grown on one horn of the PbS nanostar. The single crystallinity of the PbS stars is further confirmed by the HRTEM image shown in Fig. 1d while the crystalline nature of Au nanoparticles was confirmed by the HRTEM image shown in Fig. 1e. The related XRD pattern (Fig. 1f) shows sharp peaks corresponding to cubic PbS with a rock salt structure (JCPDS No. 5-592) and cubic gold (JCPDS No. 4-784), confirming the formation of heterodimers of PbS and Au nanocrystals.

The UV–vis absorption spectra of the PbS–Au nanostar–nanoparticle heterodimers as well as the original PbS nanostars were measured in the range of 300–1200 nm at room temperature (Fig. 2). It can be seen that the original PbS nanostars exhibited an absorption peak at ~360 nm. When Au nanoparticles were

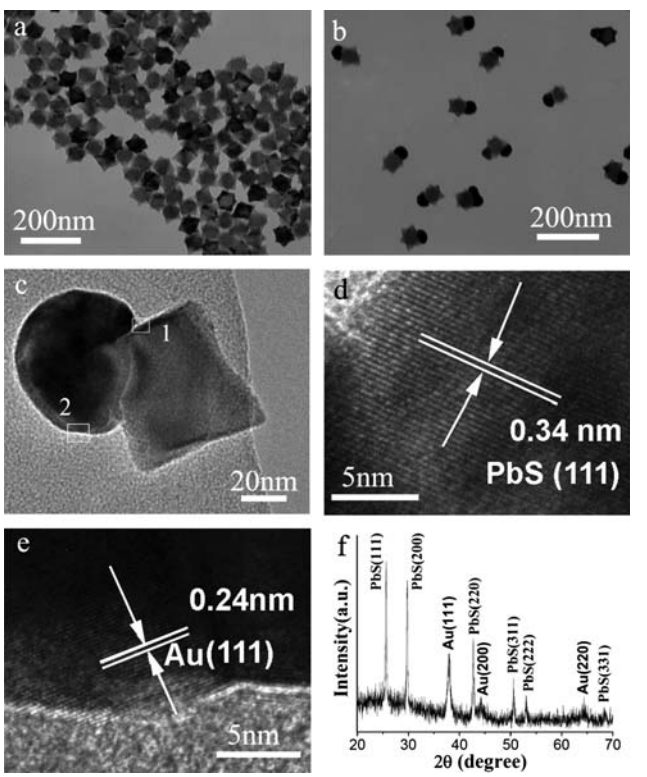

Fig. 1 (a) A TEM image of PbS nanostars. (b), (c) TEM images, (d), (e) HRTEM images and (f) XRD pattern of PbS–Au nanostar–nanoparticle heterodimers formed with [PbS] = 0.48 mM at 27 °C. The HRTEM images shown in (d) and (e) correspond to the framed areas 1 and 2 in (c), respectively.

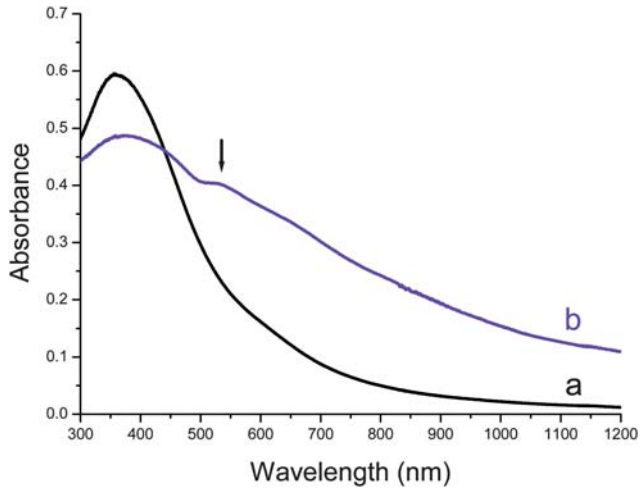

Fig. 2 UV–vis spectra of PbS nanostars (a) and PbS–Au nanostar–nanoparticle heterodimers (b). The arrow indicates the SPR peak of Au nanoparticles grown on the PbS nanostars.

grown on one horn of the PbS nanostars, the absorption peak at ~360 nm for PbS nanostars was accompanied by a shoulder at ~525 nm, which could possibly be ascribed to the surface plasmon resonance (SPR) peak of the Au nanoparticles.[35] Apparently, the absorption of the PbS–Au heterodimers essentially represents a combination of the absorption of PbS and Au. This result is in contrast to the UV–vis absorption characteristics of hollow PbS_x solid Au heterodimers, which showed the absence of an SPR peak of Au nanoparticles due to the excess sulfur in PbS_x.[19]

The size of the Au nanoparticles on the horns of the PbS nanostars could be readily adjusted by changing the PbS concentration for the deposition of Au nanoparticles. When the concentration of PbS was decreased from 0.48 mM to 0.08 mM, the size of Au nanoparticles was increased from ~50 nm to ~90 nm and the PbS nanostars were almost enclosed by the relatively large Au nanoparticles (Fig. 3a). If the PbS concentration was increased from 0.48 mM to 1.6 mM, the size of Au nanoparticles was decreased to ~30 nm (Fig. 3b).

The presence of the surfactant CTAB in the system played an important role in the formation of uniform PbS–Au nanostar–nanoparticle heterodimers. Only a small number of PbS–Au heterodimers were formed in the absence of CTAB or in the presence of a low concentration of CTAB under otherwise similar conditions. When the concentration of CTAB was moderate (0.05–0.1 M), well-defined PbS–Au nanostar–nanoparticle heterodimers formed, as shown in Fig. 1b. As the CTAB concentration was further increased, the preferential deposition of Au nanoparticles on the horn of PbS nanostars was inhibited and there appeared many bare PbS nanostars without Au deposition. Therefore, a proper CTAB concentration was essential for the selective deposition of uniform Au nanoparticles on one horn of PbS nanostars. This result might be rationalized by considering that a certain amount of CTAB adsorbed on the PbS nanostars would be favorable for the nucleation of Au nanoparticles on the horn but a much more dense CTAB adsorption layer would prevent Au deposition.

The morphology of the PbS–Au heterostructures was also influenced by the reaction temperature. When the temperature was decreased from room temperature (~27 °C) to 4 °C under otherwise identical conditions, PbS–Au nanostar–nanoparticle heterostructures consisting of Au nanoparticles made of many smaller nanocrystals were obtained (Fig. 4a). Moreover, occasionally two Au nanoparticles grew on two horns of one PbS nanostar. It may be noted that some CTAB crystals precipitated from the solution due to the low solubility of CTAB at this temperature; however, it did not show considerable effect on the preferential growth of Au nanoparticles on the horns of PbS nanostars. Nevertheless, there was a possibility that the lowered CTAB concentration somewhat contributed to the deposition of many smaller nanocrystals on the horns of PbS nanostars. When the temperature was increased to 60 °C, there was no preferential deposition of Au nanoparticles on the horn of the PbS nanostars (Fig. 4b). This result indicated that the temperature considerably affected the nucleation and growth of Au nanoparticles on the PbS nanostars.

Moreover, this method could be readily extended to the synthesis of PbS–Au nanostar–nanoparticle heterodimers using

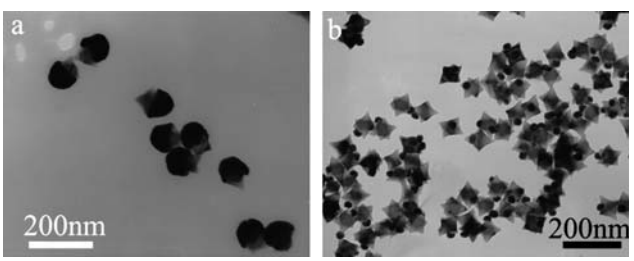

Fig. 3 TEM images of PbS–Au nanostar–nanoparticle heterodimers formed at 27 °C with different PbS concentrations: (a) 0.08 mM and (b) 1.6 mM.

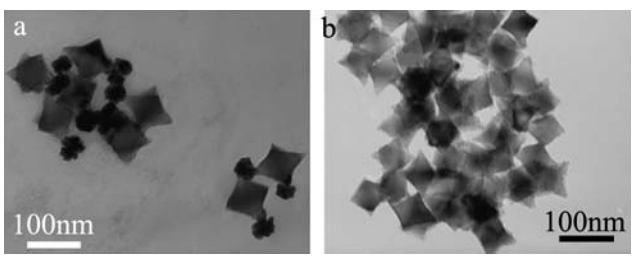

Fig. 4 TEM images of PbS–Au nanostar–nanoparticle heterostructures formed with [PbS] = 0.48 mM at 4 °C (a) and 60 °C (b).

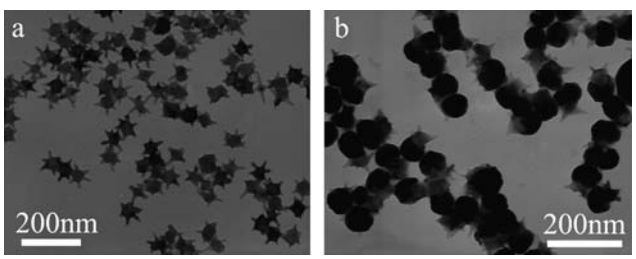

Fig. 5 TEM images of PbS nanostars with sharp horns (a) and their related PbS–Au nanostar–nanoparticle heterodimers (b).

PbS with different dimensions and morphologies as the growth template. For example, uniform PbS nanostars with sharp horns were prepared in mixed CTAB/SDS solution in the presence of ~ 0.022 M NaCl (Fig. 5a). It has been suggested that the presence of SDS would considerably accelerate the growth on the {100} faces relative to the {111} faces leading to the formation of hexapods showing six <100>-oriented arms whereas the presence of CTAB tends to just bring about a mild increase in the growth rate on the {100} faces relative to the {111} faces, which favors the formation of octahedrons showing eight {111} faces.[30] With a CTAB/SDS molar ratio of ~ 5, PbS nanostars with normal horns were obtained in the absence of additional salts. In the present situation, the presence of additional NaCl would perturb the selective adsorption of both surfactants. Presumably, the effect of the salt on the adsorption of the CTAB molecules with a higher ratio would be larger than that on the adsorption of the SDS molecules, leading to the enhancement of the role of SDS in determining the morphology of the final PbS nanocrystals. As a result, PbS nanostars with much sharper <100>-oriented horns were obtained. The obtained sharp-horned PbS nanostars were subsequently used as the growth templates for the selective deposition of Au nanoparticles, resulting in the formation of PbS–Au nanostar–nanoparticle heterodimers (Fig. 5b).

Apparently, the formation of the PbS–Au nanostar–nanoparticle heterodimers was achieved through selective deposition of one Au nanoparticle onto one horn of the PbS nanostars. The specificity of the selective tip growth could be ascribed to preferential Au deposition onto the PbS horns. The horns were more reactive because of the increased surface energy of sharp tips; meanwhile, there could be imperfect adsorption of the surfactants on the horns since the six horns grew the fastest and there were the least surfactant molecules capping the horns, which could also contribute to the higher reactivity of the horns. For these reasons, the horns became the specific sites for the nucleation and growth of Au nanoparticles. As long as the nucleation of Au nanoparticles occurred on one horn of the PbS nanostars, the nucleation of Au nanoparticles on the other five horns could be prevented due to the relatively high activation energy required for heterogeneous nucleation. Then, a continuous growth of the Au nanoparticles nucleated on one horn of the PbS nanostars resulted in the formation of the unique PbS–Au nanostar–nanoparticle heterodimers. Another possibility for the selective Au deposition on one horn is that Au nanoparticles initially deposited on all the six horns, which subsequently underwent Ostwald ripening, leading to the continuous growth of one Au nanoparticle with the other five Au nanoparticles gradually dissolved. However, more detailed investigations are required to elucidate the exact mechanism of the selective growth of Au nanoparticles on one horn of PbS nanostars. It may be noted that gold encapsulation of FePt nanostars was recently achieved by a similar seeded-growth method.[36] Owing to the affinity between the two noble metals Pt and Au, the growth of a uniform Au shell on the surface of the FePt nanostars occurred. In contrast, Au nanoparticles were preferentially grown on the horns of the PbS nanostars in the current situation, which could be largely ascribed to the chemical and structural differences between PbS and Au.

Since PbS nanocrystals can be readily dissolved or etched in acidic solutions, PbS–Au nanoframe–nanoparticle heterodimers and cap-like Au nanoparticles can be obtained by etching the PbS–Au nanostar–nanoparticle heterodimers with different acids. As shown in Fig. 6, unusual PbS–Au nanoframe–nanoparticle heterodimers were obtained after etching the PbS–Au nanostar–nanoparticle heterodimers using 0.05 M oxalic acid. The SEM image shown in Fig. 6a suggests that the original six-horn PbS nanostars were carved into star-shaped nanoframes, which looked like concaved octahedral with eight highly symmetric cavities enclosed by nanoflakes. The corresponding TEM image shows that there was still one Au nanoparticle capping one horn of the star-shaped PbS nanoframe (Fig. 6b). The HRTEM image shown in Fig. 6c clearly shows that the nanoframe–nanoparticle heterodimers consisted of polycrystalline Au nanoparticles grown on one horn of the single-crystalline star-shaped PbS nanoframe. The formation of the star-shaped PbS nanoframes consisting of nanoflakes due to the selective etching of PbS nanostars was unexpected. Our preliminary experiments showed that the etching of pure PbS nanostars with various acids usually started from the six horns and hence star-shaped PbS nanoframes could not be obtained. When a Au nanoparticle was grown on one horn of the PbS nanostar, the etching of the PbS nanostar started from the eight concaved surfaces instead of the six horns, leading to the formation of the final PbS–Au nanoframe–nanoparticle heterodimer. The exact mechanism for this unique phenomenon is still unknown, but is certainly worthy of further investigation.

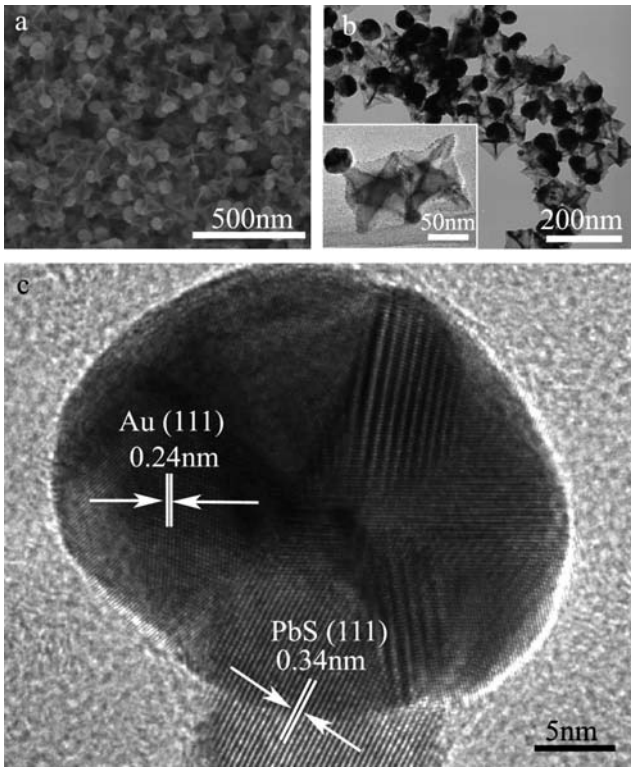

Fig. 6 SEM (a), TEM (b), and HRTEM (c) images of PbS–Au nanoframe–nanoparticle heterodimers obtained by etching the PbS–Au nanostar–nanoparticle heterodimers formed with [PbS] = 0.48 mM using 0.05 M oxalic acid.

It could be expected that complete removal of PbS nanostars from the PbS–Au nanostar–nanoparticle heterodimers would

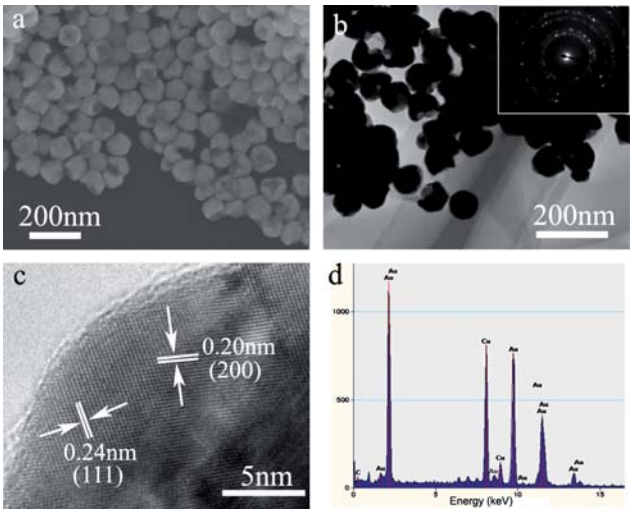

Fig. 7 SEM (a), TEM (b), and HRTEM (c) images and EDS spectrum (d) of cap-like Au nanoparticles obtained by etching the PbS–Au nanostar–nanoparticle heterodimers formed with [PbS] = 0.08 mM using 6 M HCl. The inset shows the related ED pattern.

result in cap-like Au nanoparticles with a carved cavity. Actually, this kind of cap-like Au nanoparticle was obtained through corrosion of the PbS–Au nanostar–nanoparticle heterodimers using 6 M hydrochloric acid. Fig. 7a shows a representative SEM image of the obtained cap-like Au nanoparticles. It is obvious that the obtained Au nanoparticles had a cross-shaped cavity carved by the sharp horn of the PbS nanostars, which faithfully replicated the shape of the horn of a six-armed star. The TEM image and the related electron diffraction (ED) pattern confirmed the formation of the cap-like Au nanoparticles with a carved cavity (Fig. 7b). The HRTEM and the energy-dispersive X-ray spectroscopy (EDS) characterization provided further support for the formation of pure Au crystals (Fig. 7c and d). It may be noted that Au nanocaps or semishells with a round cavity have been fabricated using polystyrene spheres as a template;[34] however, the fabrication of Au nanocaps with a cavity of a complex morphology has been difficult to realize. The current Au nanocaps with a cross-shaped cavity could provide promising anisotropic building blocks for self-assembly, and they might show novel plasmonic and optical properties owing to their unique morphology. However, considerable aggregation of the Au nanocaps in solution took place during etching of the PbS nanostars (as shown in Fig. 7b), which prevented us from obtaining reproducible absorption spectra of the Au nanocaps. Further work is under way to obtain well-dispersed Au nanocaps and to characterize their optical properties. To summarize, unusual PbS–Au nanoframe–nanoparticle heterodimers and cap-like Au nanoparticles can be readily obtained by controlled etching of the PbS–Au nanostar–nanoparticle heterodimers, which were prepared by selective deposition of Au nanoparticles on the PbS nanostars, using different acids (Scheme 1).

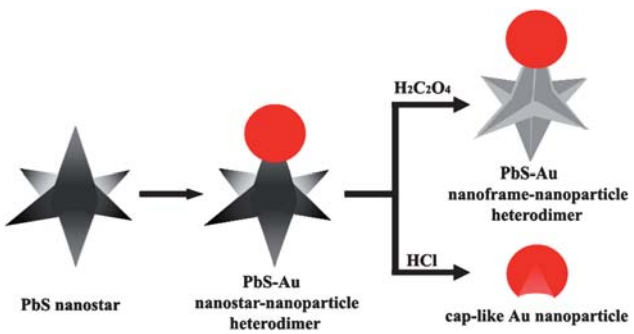

Scheme 1 Schematic illustration of the formation of a PbS–Au nanostar–nanoparticle heterodimer and its transformation into a PbS–Au nanoframe–nanoparticle heterodimer and cap-like Au nanoparticle by acid etching.

Conclusions

In summary, uniform PbS–Au nanostar–nanoparticle heterodimers consisting of one Au nanoparticle grown on one horn of a well-defined six-horn PbS nanostar were prepared using PbS nanostars as the growth substrates for selective deposition of Au nanoparticles. The size of the Au nanoparticles on the horns of the PbS nanostars could be readily adjusted by changing the PbS concentration for the deposition of Au nanoparticles. An optimum CTAB concentration and temperature were essential for the selective deposition of uniform Au nanoparticles on one horn of a PbS nanostar. Unusual PbS–Au nanoframe–nanoparticle heterodimers were obtained by etching the PbS–Au nanostar–nanoparticle heterodimers with oxalic acid while novel cap-like Au nanoparticles were obtained by etching with hydrochloric acid. The obtained heterodimeric nanostructures and cap-like nanoparticles are promising candidates for anisotropic nanoscale building blocks for the controllable assembly of useful, complex architectures. The synthetic method based on aqueous solution is very simple, low-cost, and extendable to the synthesis of hybrid nanostructures with other compositions. This result would facilitate the potential applications of complex nanocrystal-based heterostructures in assembly and integration into functional device architectures.

Acknowledgements

Financial support from NSFC (Grants 20873002, 20633010, and 50821061), MOST (Grant 2007CB936201), and SRFDP (Grant 20070001018) is gratefully acknowledged.

References

1 T. K. Sau and A. L. Rogach, *Adv. Mater.*, 2010, **22**, 1781.
2 Y. Xia, Y. Xiong, B. Lim and S. E. Skrabalak, *Angew. Chem., Int. Ed.*, 2009, **48**, 60.
3 A. R. Tao, S. Habas and P. Yang, *Small*, 2008, **4**, 310.
4 M. Grzelczak, J. Pérez-Juste, P. Mulvaney and L. M. Liz-Marzán, *Chem. Soc. Rev.*, 2008, **37**, 1783.
5 Y.-W. Jun, J.-S. Choi and J. Cheon, *Angew. Chem., Int. Ed.*, 2006, **45**, 3414.
6 L. Qi, *Coord. Chem. Rev.*, 2010, **254**, 1054.
7 P. D. Cozzoli, T. Pellegrino and L. Manna, *Chem. Soc. Rev.*, 2006, **35**, 1195.
8 Y. W. Jun, J. S. Choi and J. Cheon, *Chem. Commun.*, 2007, 1203.
9 T. Mokari, E. Rothenberg, I. Popov, R. Costi and U. Banin, *Science*, 2004, **304**, 1787.
10 C. Pacholski, A. Kornowski and H. Weller, *Angew. Chem., Int. Ed.*, 2004, **43**, 4774.

11 R. Costi, A. E. Saunders and U. Banin, *Angew. Chem., Int. Ed.*, 2010, **49**, 4878.
12 H. W. Gu, R. K. Zheng, X. X. Zhang and B. Xu, *J. Am. Chem. Soc.*, 2004, **126**, 5664.
13 (*a*) H. Zeng and S. H. Sun, *Adv. Funct. Mater.*, 2008, **18**, 391; (*b*) C. Wang, C. J. Xu, H. Zeng and S. H. Sun, *Adv. Mater.*, 2009, **21**, 3045.
14 (*a*) T. Pellegrino, A. Fiore, E. Carlino, C. Giannini, P. D. Cozzoli, G. Ciccarella, M. Respaud, L. Palmirotta, R. Cingolani and L. Manna, *J. Am. Chem. Soc.*, 2006, **128**, 6690; (*b*) A. Figuerola, A. Fiore, R. D. Corato, A. Falqui, C. Giannini, E. Micotti, A. Lascialfari, M. Corti, R. Cingolani, T. Pellegrino, P. D. Cozzoli and L. Manna, *J. Am. Chem. Soc.*, 2008, **130**, 1477.
15 R. Klajn, A. O. Pinchuk, G. C. Schatz and B. A. Grzybowski, *Angew. Chem., Int. Ed.*, 2007, **46**, 8363.
16 J. Shin, H. Kim and I. S. Lee, *Chem. Commun.*, 2008, 5553.
17 J. Choi, Y. Jun, S. Yeon, H. C. Kim, J. S. Shin and J. Cheon, *J. Am. Chem. Soc.*, 2006, **128**, 15982.
18 J. Yang, H. I. Elim, Q. B. Zhang, J. Y. Lee and W. Ji, *J. Am. Chem. Soc.*, 2006, **128**, 11921.
19 S. Huang, J. Huang, J. Yang, J.-J. Peng, Q. Zhang, F. Peng, H. Wang and H. Yu, *Chem.–Eur. J.*, 2010, **16**, 1449.
20 (*a*) C. Xu, J. Xie, H. Don, C. Wang, N. Kohler, E. G. Walsh, J. R. Morgan, Y. E. Chin and S. Sun, *Angew. Chem., Int. Ed.*, 2008, **47**, 173; (*b*) C. Xu, B. Wang and S. Sun, *J. Am. Chem. Soc.*, 2009, **131**, 4216.
21 J. Jiang, H. Gu, H. Shao, E. Devlin, G. C. Papaefthymiou and J. Y. Ying, *Adv. Mater.*, 2008, **20**, 4403.
22 T. Hirakawa and P. V. Kamat, *J. Am. Chem. Soc.*, 2005, **127**, 3928.
23 H. Y. Lin, Y. F. Chen, J. G. Wu, D. I. Wang and C. C. Chen, *Appl. Phys. Lett.*, 2006, **88**, 161911.
24 T. Mokari, C. G. Sztrum, A. Salant, E. Rabani and U. Banin, *Nat. Mater.*, 2005, **4**, 855.
25 R. Costi, A. E. Saunders, E. Elmalem, A. Salant and U. Banin, *Nano Lett.*, 2008, **8**, 637.
26 S. C. Glotzer and M. J. Solomon, *Nat. Mater.*, 2007, **6**, 557.
27 S. M. Lee, Y. W. Jun, S. N. Cho and J. Cheon, *J. Am. Chem. Soc.*, 2002, **124**, 11244.
28 K. Roy Choudhury, Y. Sahoo, S. J. Jang and P. N. Prasad, *Adv. Funct. Mater.*, 2005, **15**, 751.
29 J. P. Ge, J. Wang, H. X. Zhang, X. Wang, Q. Peng and Y. D. Li, *Chem.–Eur. J.*, 2005, **11**, 1889.
30 N. Zhao and L. Qi, *Adv. Mater.*, 2006, **18**, 359.
31 (*a*) S. A. McDonald, G. Konstantatos, S. G. Zhang, P. W. Cyr, E. J. D. Klem, L. Levina and E. H. Sargent, *Nat. Mater.*, 2005, **4**, 138; (*b*) G. Konstantatos, I. Howard, A. Fischer, S. Hoogland, J. Clifford, E. Klem, L. Levina and E. H. Sargent, *Nature*, 2006, **442**, 180.
32 (*a*) C. J. Murphy, A. M. Gole, J. W. Stone, P. N. Sisco, A. M. Alkilany, E. C. Goldsmith and S. C. Baxter, *Acc. Chem. Res.*, 2008, **41**, 1721; (*b*) S. E. Skrabalak, J. Chen, Y. Sun, X. Lu, L. Au, C. M. Cobley and Y. Xia, *Acc. Chem. Res.*, 2008, **41**, 1587; (*c*) S. K. Ghosh and T. Pal, *Chem. Rev.*, 2007, **107**, 4797; (*d*) R. Wilson, *Chem. Soc. Rev.*, 2008, **37**, 2028.
33 (*a*) N. Zhao, Y. Wei, N. Sun, Q. Chen, J. Bai, L. Zhou, Y. Qin, M. Li and L. Qi, *Langmuir*, 2008, **24**, 991; (*b*) Y. Qin, Y. Song, N. Sun, N. Zhao, M. Li and L. Qi, *Chem. Mater.*, 2008, **20**, 3965; (*c*) T. Huang, F. Meng and L. Qi, *Langmuir*, 2010, **26**, 7582; (*d*) L. Li, Z. Wang, T. Huang, J. Xie and L. Qi, *Langmuir*, 2010, **26**, 12330.
34 (*a*) J. Liu, A. I. Maaroof, L. Wieczorek and M. B. Cortie, *Adv. Mater.*, 2005, **17**, 1276; (*b*) J. Ye, N. Verellen, W. V. Roy, L. Lagae, G. Maes, G. Borghs and P. Van Dorpe, *ACS Nano*, 2010, **4**, 1457.
35 J. Zhang, J. Du, B. Han, Z. Liu, T. Jiang and Z. Zhang, *Angew. Chem., Int. Ed.*, 2006, **45**, 1116.
36 N. Pazos-Pérez, B. Rodríguez-González, M. Hilgendorff, M. Giersigb and L. M. Liz-Marzán, *J. Mater. Chem.*, 2010, **20**, 61.